Nucl. Sci. and Tech., Vol.14, No. 2 (2024), pp. 40-55

Nuclear Science and Technology

Journal homepage: http://jnst.vn/index.php/nst

# Synthesizing high-density $U_3O_8$ powder from $UO_2F_2$ solution via AUC precipitation

Nguyen Trong Hung and Nguyen Thanh Thuy

*Institute for Technology of Radioactive and Rare Elements*
*Address: 48-Lang Ha, Dong Da, Hanoi, Vietnam*
**Corresponding email: nthungvaec@gmail.com*

**Abstract:** Uranium trioxide octaoxide compound - $U_3O_8$ is a crucial nuclear material in nuclear technology. It is used as nuclear fuel for research reactors. To achieve this goal, an important characteristic that $U_3O_8$ powder must possess is a density ranging from 88-98% of the theoretical density (TD). This paper reports the results of an investigation of the ammonium uranyl carbonate (AUC) precipitation from uranyl fluoride ($UO_2F_2$) solution and optimization of sintering parameters for synthesizing high-density $U_3O_8$ powder, meeting the specified standards for manufacturing dispersed nuclear fuel for research reactors. The AUC precipitation was conducted using uranyl fluoride ($UO_2F_2$) solutions with uranium concentrations ranging from 80 to 120 $gL^{-1}$ and ammonium carbonate ($(NH_4)_2CO_3$) concentrations as precipitant were maintained between 200 and 400 $gL^{-1}$, while the $(NH_4)_2CO_3$ to U (C/U) molar ratios were kept equal to or greater than 6. The investigated parameters for sintering of the high-density $U_3O_8$ nuclear material derived from AUC (ex-AUC $U_3O_8$) are the sintering temperature and time. The experimental studies are designed by using the Response Surface Methodology (RSM) based on a Central Composite Design (CCD). As a result, a regression equation describing the dependency of $U_3O_8$ powder density on sintering temperature and time has been established. Based on this equation, the sintering for synthesizing high-density $U_3O_8$ powder has been optimized. The regression equation aids in controlling the parameters of the $U_3O_8$ powder sintering.

**Keywords:** *Uranyl ammonium carbonate (AUC), triuranium octaoxide ($U_3O_8$), nuclear material, nuclear research reactor.*

## I. INTRODUCTION

Research nuclear reactors have numerous applications across various economic and societal sectors. They serve as unique tools for producing specialized materials (e.g., silicon irradiation for semiconductor production-neutron transmutation doping technology), isotopes, and radiopharmaceuticals (e.g., Ac-255 isotope, Y-90 microspheres for liver cancer treatment, Tc-99m, etc.), as well as for fundamental research, neutron-activation analysis, and materials testing [1].

The fuel for research reactors typically exists in the form of U-Si (or U-Mo) alloys dispersed in an aluminum matrix (in metmet form) or $U_3O_8$ (or $UO_2$) ceramic powder dispersed in an aluminum matrix (in cermet form). The fuel used in research reactors contains a higher level of enrichment, usually around 20% at present, compared to the fuel utilized in power reactors. This type of fuel, known as low-enriched uranium (LEU), is characterized by a lower presence of U-238. Consequently, the resulting used fuel exhibits reduced amounts of actinides and lower heat generation from radioactive decay. The composition of fission products in this fuel is comparable to that found in used power reactor fuel. Fuel assemblies for research reactors typically consist of plates or cylinders made from a uranium-aluminium alloy (U-Al) and

https://doi.org/10.53747/nst.v14i2.455
Received 07 January 2024, accepted 21 June 2024

clad with pure aluminium. This design differs from the ceramic $UO_2$ pellets enclosed in Zircaloy cladding commonly employed in power reactors. Despite being more highly enriched, only a few kilograms of uranium are required to fuel a research reactor, in contrast to the approximately hundred tonnes needed for a power reactor. Research reactors commonly function at low temperatures, with the coolant maintained below 100ºC. However, the operating conditions present their own set of challenges. In comparison to power reactor fuel, which operates at a power density of approximately 5 $kWcm^{-3}$, research reactor fuel may experience a higher power density, reaching up to 17 $kWcm^{-3}$ within the fuel meat. Additionally, the burnup in research reactors is significantly greater, necessitating fuel that can endure structural damage from fission and accommodate a larger quantity of fission products [2].

The initial research reactors constructed in the 1940s were characterized by low power and primarily served for investigating reactor physics and reactor technology. In the subsequent decades of the 1950s and 1960s, research reactors with low power were established globally, utilizing fuel enriched with uranium up to 20% or less of U-235 by weight (LEU). This enrichment level was selected based on the belief that it provided a sufficient barrier to prevent the use of U-235 for nuclear weapons. It is feasible to decrease the enrichment of fuel in many research and test reactor designs, provided that the U-235 content in the fuel element is maintained at approximately the same level, despite the reduced enrichment. In reality, it becomes necessary to augment the U-235 content of the fuel to offset the reduction in reactivity resulting from the heightened neutron absorption by the presence of U-238. The conversion from high-enriched uranium (HEU) to LEU fuel (belonging to programme for Reduced Enrichment for Research and Test Reactors-RERTR) requires an increase in the uranium density in the fuel. While the uranium density in HEU fuel is only about 1.3-1.7 $gcm^{-3}$ of uranium, the LEU fuel needs to achieve a density of 2.3-3.2 $gcm^{-3}$ of uranium. Therefore, specifically for LEU fuel in the form of $U_3O_8$+Al, $U_3O_8$ nuclear fuel powder must have a high density to meet the designed uranium density in the LEU fuel [3].

The technology for synthesizing high-density $U_3O_8$, especially designed for manufacturing LEU nuclear fuel for research reactors, has not been widely published. According to some documents, the methods in this technology include [4-7]:

(i) Starting from uranium hexafluoride compound – $UF_6$ after the process of U-235 isotope enrichment:

The $UF_6$ compound, enriched to approximately 20% of U-235, will undergo hydrolysis to form a solution system of uranyl fluoride + hydrofluoric acid – $UO_2F_2$+HF, following the reaction:

$$UF_6 + 2H_2O \rightarrow UO_2F_2 + 4HF \quad (1)$$

Thus, the $UO_2F_2$ to HF molar ratio in the hydrolysis solution of $UF_6$ is 1 to 4. From this hydrolysis solution, uranium will be precipitated as either uranyl peroxide – $UO_4$ or ammonium uranyl carbonate – AUC in the form of crystals and spherical particles (the form of ammonium diuranate – ADU is less commonly used due to its non-stoichiometric precipitation and fine crystalline structure). The precipitation reactions of $UO_4$ and AUC are as follows:

$$UO_2F_2 + H_2O_2 \rightarrow UO_2O_2 + 2HF \quad (2)$$

$$UO_2F_2 + 3(NH_4)_2CO_3 \rightarrow UO_2CO_3.2(NH_4)_2CO_3 + 2NH_4F \quad (3)$$

From the precipitate of $UO_4$ or AUC, it is calcinated in a low nitrogen environment ($N_2$) at 800ºC in an electric furnace; subsequently, it undergoes further sintering at a high-temperature of 1400ºC, in electric

furnace and in a low nitrogen environment, to stabilize the density.

(ii) Starting from metallic uranium:

The $UF_6$ compound, enriched to approximately 20% of U-235, will undergo the reduction in a hydrogen ($H_2$) atmosphere to yield uranium tetrafluoride – $UF_4$, which follows the reaction:

$$UF_6 + H_2 \rightarrow UF_4 + 2HF \quad (4)$$

From the $UF_4$ compound, it will be metallothermically reduced by using calcium (Ca) or magnesium (Mg) as a reductant to produce metallic uranium. The reduction metallothermic reaction using calcium (or magnesium) is as follows:

$$UF_4 + 2Ca(Mg) \rightarrow U + 2Ca(Mg)F_2 \quad (5)$$

The metallic uranium obtained from the transformation of $UF_6$ to $UF_4$ and its metallothermic reduction is then subjected to combustion to form $U_3O_8$. The combustion reaction of the metallic uranium is carried out in an electric furnace and in an air environment. Towards the end of the combustion, additional oxygen is introduced to ensure complete transformation into $U_3O_8$:

$$3U + 4O_2 \rightarrow U_3O_8 \quad (6)$$

In these reactions, oxygen ($O_2$) is used to oxidize the metallic uranium to uranium oxides, and further oxidation results in the formation of $U_3O_8$, a most stable oxide form of uranium.

(iii) Starting from the nitrate solution resulted in the spent nuclear fuel reprocessing:

In a continuous denitration, nitrates ion is separated from the uranyl nitrate solution – $UO_2(NO_3)_2$ to form uranium trioxide – $UO_3$. This oxide is then further heated at 800$^o$C in an electric furnace in a low nitrogen atmosphere to convert it into $U_3O_8$ powder.

The $U_3O_8$ powder used in the fabrication of dispersed nuclear fuel plates for research reactors needs to reach a density $d \geq 7.4\times10^3$ kgm$^{-3}$ (TD of $U_3O_8$ $d=8.4\times10^3$ kgm$^{-3}$) to meet the designed uranium density in the LEU fuel core [8-10]. This paper reports on the technique for synthesizing high-density $U_3O_8$ powder from $UO_2F_2$+HF solution system via the AUC compound precipitation.

## II. MATERIALS AND METHODS

### A. Materials

In the conducted experiments, the precipitants employed, specifically ammonium carbonate and ammonium hydroxide, were of superior commercial purity, with a minimum of 99%, and were procured from Shanghai Epoch Material Co., Ltd. The uranyl nitrate solution is originated from nuclear-grade pregnant stripping liquor acquired through Vietnam's yellow cake purification extraction method [11-12]. This extraction was internally conducted by the Institute for Technology of Radioactive and Rare Elements, a division of the Vietnam Atomic Energy Institute, employing tributyl phosphate as a standard solvent in uranium extraction.

### B. Preparing $UO_2F_2$+HF solution system

The process of preparing a simulated solution for the $UF_6$ hydrolysis, in the form of the $UO_2F_2$+HF solution with a $UO_2F_2$ to HF molar ratio of 1 to 4, was carried out, including the following steps:

(i) Firstly, the uranyl nitrate solution obtained after the refinement of Vietnam's yellowcake ($U_3O_8$) by the solvent extraction method using Tri Butyl Phosphate-TBP as a extractant is crystallized into uranyl nitrate hexahydrate crystals - $UO_2(NO_3)_2.6H2O$ (UNH). The crystallization is carried out by slow evaporation of the uranyl nitrate solution with a uranium concentration of approximately 100 gL$^{-1}$ at a temperature of 90°C. After the appearance of crystal foam, the crystallization is halted overnight to obtain UNH crystals. Subsequently, the UNH crystals are collected, and the uranyl nitrate solution is

replenished to continue the crystallization for the subsequent batch.

(ii) The UNH salt crystals are dissolved in absolute alcohol, and then the solution is evaporated. The $NO_3^-$ ions are reduced to form ethylnitrate – $C_2H_5ONO_2$ with a boiling point of 88.7°C. The evaporation is slow, resulting in the precipitation of uranyl hydroxide – $UO_2(OH)_2$.

It should be noted that in the process of preparing $UO_2(OH)_2$, the formation of ethylnitrate occurs. This compound is highly flammable and explosive, so the procedure must be conducted with a high level of expertise and caution.

(iii) Uranyl hydroxide is readily dissolved in HF acid solution, forming a solution with the composition of $UO_2F_2$+HF with an HF to $UO_2F_2$ molar ratio of 4; this solution simulates the hydrolysis of $UF_6$.

The contents of various impurities in the $UO_2F_2$+HF solution, as shown in Table I, satisfy the standards of ASTM C788-3: Impurity Limits in Uranyl Nitrate for Direct Conversion to Oxide.

**Table I.** The contents of various impurities in the $UO_2F_2$+HF solution

| Impurity | Concentration* (ppm) | Content (μg/g U) | ASTM C788-3 (μg/g U) |
|---|---|---|---|
| Aluminum | 13 | 88 | 150 |
| Calcium + Magnesium | 17 | 116 | 150 |
| Iron | 25 | 174 | 200 |
| Manganese | 23 | 156 | 200 |
| Zinc | 20 | 135 | 200 |

** Uranium concentration in the $UO_2F_2$+HF solution is 145gL$^{-1}$*

### C. Procedure for the AUC precipitation from $UO_2F_2$+HF precursor solution

To initiate the AUC precipitation from the $UO_2F_2$+HF precursor solution, $(NH_4)_2CO_3$ solutions with concentrations ranging from 200 to 400 gL$^{-1}$ were utilized as the precipitant. Concurrently, a 1.0 M $NH_4OH$ solution was applied to neutralize the acidic solution. The precipitation was executed in batches, wherein a fixed quantity of $UO_2F_2$+HF precursor solution, featuring a predetermined uranium concentration (80, 100, or 120 gL$^{-1}$), was blended with a specific volume of $(NH_4)_2CO_3$ solution. The $UO_2F_2$+HF feedstocks were introduced into a plastic beaker, which contained a sufficient amount of 1.0 M $NH_4OH$ solution to neutralize the HF acid present in the $UO_2F_2$+HF precursor solution, as indicated by the following reaction:

$$HF + NH_4OH = NH_4F + H_2O \quad (7)$$

Concurrently, an established concentration of $(NH_4)_2CO_3$ precipitant was introduced into the reaction beaker using another metering pump. Throughout most AUC precipitation experiments, the stirring speed was consistently maintained at approximately 100 rpm, and the precipitation duration extended beyond 4 hours. The precipitation underwent meticulous monitoring and control to ensure the complete precipitation of soluble uranium within the reaction beaker. The resultant AUC slurry underwent an overnight aging treatment to facilitate thorough settling and enhance the purity of the AUC product. Following the aging, the precipitate underwent filtration and thorough washing with absolute ethanol. Subsequently, the wet AUC cake underwent heating in an oven at 70°C for 5 hours. This thermal treatment

effectively removed water and liberated ammonium carbonate, resulting in the production of a highly pure AUC product with the desired composition. This product is now prepared for subsequent processing.

### D. Sintering of AUC powder into high-density $U_3O_8$ powder

A Nabertherm tube furnace with a maximum operating temperature of 1800°C was employed for the sintering of AUC powder to produce high-density $U_3O_8$ powder. The dried AUC powder was meticulously arranged within the furnace for the sintering operation. Rigorous monitoring was undertaken to ensure the maintenance of optimal conditions throughout the entire sintering.

### E. Characterization of the AUC and $U_3O_8$ powders

X-ray diffraction (XRD) analysis was executed using a Siemens D5005 instrument equipped with monochromatized Cu Kα radiation (λ = 0.15418 nm) to evaluate the quality and crystal phases of the samples. This method offers valuable insights into the crystal structure and purity of the examined samples. For a comprehensive understanding of the composition, purity, and thermal stability of the AUC samples, thermogravimetric analysis (TGA) and differential thermal analysis (DTA) were carried out using a SETARAM thermal analyzer. Scanning electron microscopy (SEM) using a JEOL-IT100LV instrument from Horiba, Japan, was employed to visualize the morphology of both AUC and $U_3O_8$ powders. Additionally, laser scattering methods were utilized with a PARTICA LA-960 instrument (Horiba, Japan) to determine the particle size distributions of the powders. The integration of these analytical techniques provided a thorough understanding of the characteristics of AUC and $U_3O_8$ powders, facilitating the optimization of both the process and material properties.

## III. RESULTS AND DISCUSSION

### A. Study on the AUC precipitation

Eung Ho Kim and colleagues [13] conducted a detailed study on the influence of uranium concentration in $UO_2(NO_3)_2$ solution and the concentration of $(NH_4)_2CO_3$ precipitant on the morphology and chemical composition of the AUC precipitate. They observed that the shape of the AUC precipitate varied under different conditions. When the uranium concentration exceeds 80 $gL^{-1}$ and the $(NH_4)_2CO_3$ concentration is higher than 200 $gL^{-1}$, with a molar ratio of $(NH_4)_2CO_3$/U (C/U) greater than 5 and a pH above 7.6, a well-defined AUC precipitate is determined. In the concentration range of $(NH_4)_2CO_3$ from 80-120 $gL^{-1}$, the molar ratio of C/U from 4 to 5, and the pH from 7.3 to 7.5, the AUC precipitate takes on a needle-like form. On the contrary, for $(NH_4)_2CO_3$ concentrations ranging from 60 $gL^{-1}$ to 80 $gL^{-1}$, with a molar ratio of C/U fluctuating between 3.5 and 4.0, and a pH from 7.0 to 7.3, the AUC precipitate exhibits a leaf-like form. These results emphasize the significant influence of uranium and $(NH_4)_2CO_3$ concentrations on the morphology and composition of the AUC precipitate. Finally, it has been observed that when the $(NH_4)_2CO_3$ concentration falls within the range of 40-60 $gL^{-1}$, with a molar ratio of C/U less than 3.5 and a pH below 4.0, the AUC precipitate takes on an uneven form. To gain a deeper understanding of the chemical composition and structure of these precipitates, X-ray diffraction (XRD), infrared spectroscopy (IR), and thermal analysis techniques have been employed. The results have confirmed that the crystal structure of the well-defined AUC precipitate has been determined to have the formula $(NH_4)_4UO_2(CO_3)_3$. The crystal structures in a rectangular form correspond to the crystal structure of ammonium uranate. In contrast, AUC precipitates in needle-like and leaf-like forms exhibit almost no crystal structure, lacking clear crystallographic arrangements. However, the well-defined AUC precipitate shows a relatively high degree of crystallinity,

which is advantageous for the filtration or removal of dissolved impurities in subsequent processing steps.

In a separate study conducted by Boualia and colleagues [14], the influence of excess $(NH_4)_2CO_3$ on the uranium concentration in the solution of AUC precipitate leaching was examined. The researchers found that as the excess $(NH_4)_2CO_3$ in the solution increased, there was a corresponding decrease in the uranium concentration in the solution of AUC precipitate leaching. This reduction ultimately leads to the complete crystallization of the AUC precipitate. Additionally, the researchers also noted a significant decrease in the solubility of the AUC precipitate in the range of $(NH_4)_2CO_3$ concentrations from 200 $gL^{-1}$ to 400 $gL^{-1}$. These results indicate that the presence of excess $(NH_4)_2CO_3$ plays a crucial role in promoting the precipitation and crystallization of AUC, while simultaneously reducing its solubility in the solution.

Based on the literature review, experimental conditions for the AUC precipitation have been determined. The uranium concentration in the $UO_2F_2$ solution has been chosen in the range of 80 $gL^{-1}$ to 120 $gL^{-1}$, while the precipitant $(NH_4)_2CO_3$ concentration is selected in the range of 200 $gL^{-1}$ to 400 $gL^{-1}$; the C/U ratio is chosen to be ≥ 6, from 6 to 9. By controlling these parameters, the AUC precipitation will achieve the desired results and support the subsequent transformation into $U_3O_8$ powder with the desired characteristics. Experimental results have indicated that, under the described precipitation conditions, the AUC precipitate crystallizes in a well-defined form with the formula $(NH_4)_4UO_2(CO_3)_3$ (as in reaction equation 3). In Figs. 1, the X-ray diffraction (XRD) pattern illustrates the AUC powder precipitated at a C/U ratio of 6 and 7, and 8 and 9, respectively. The pattern reveals a distinct peak at 2θ = 14°, indicative of AUC with a monoclinic structure (space group *C2/c*). The lattice constants are determined as a=b=10.06(1) Å and c=12.86(2) Å, with angles α=γ=90° and β=96.42°. These findings align with prior reports [15-17], underscoring the accuracy and consistency of the observed AUC crystal structures. Additionally, Fig. 2 presents a SEM micrograph depicting a representative AUC crystal.

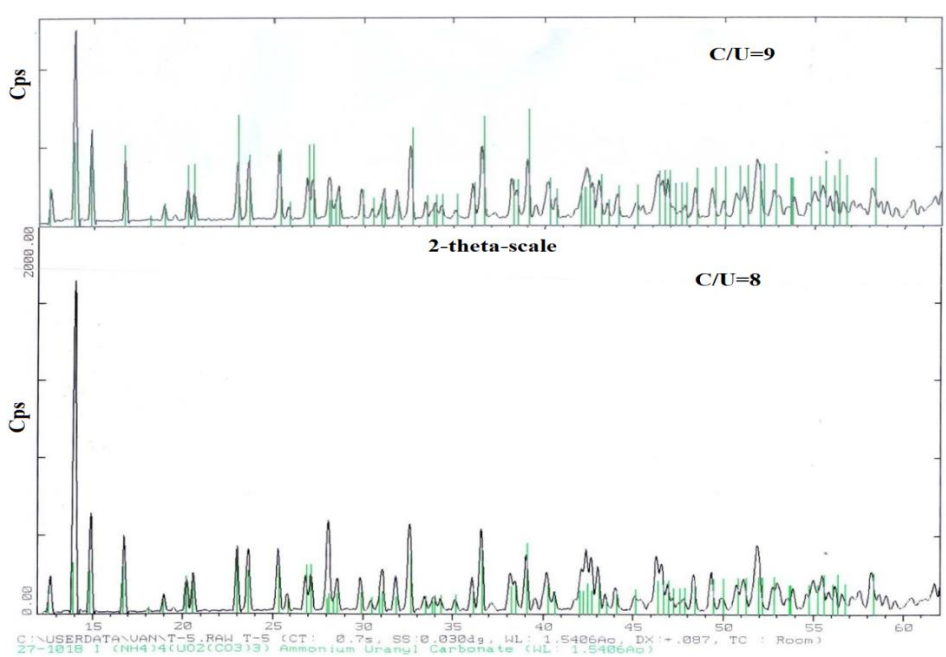


**Fig. 1a.** XRD spectrum of AUC precipitated at C/U of 8 and 9

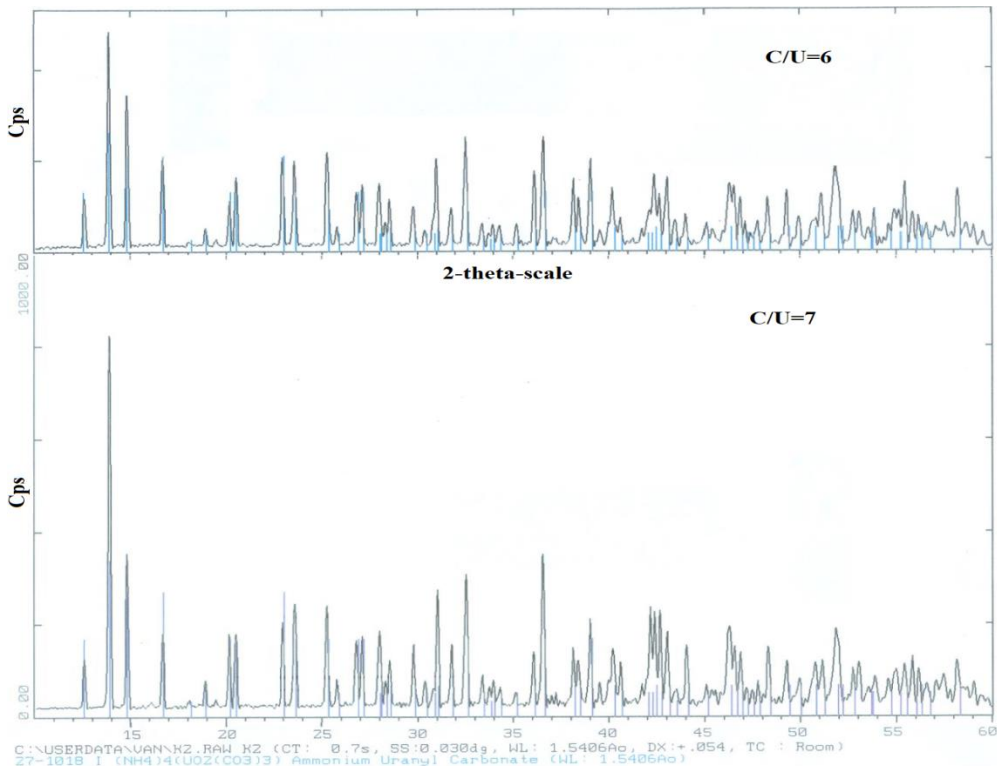


**Fig. 1b.** XRD spectrum of AUC precipitated at C/U of 6 and 7

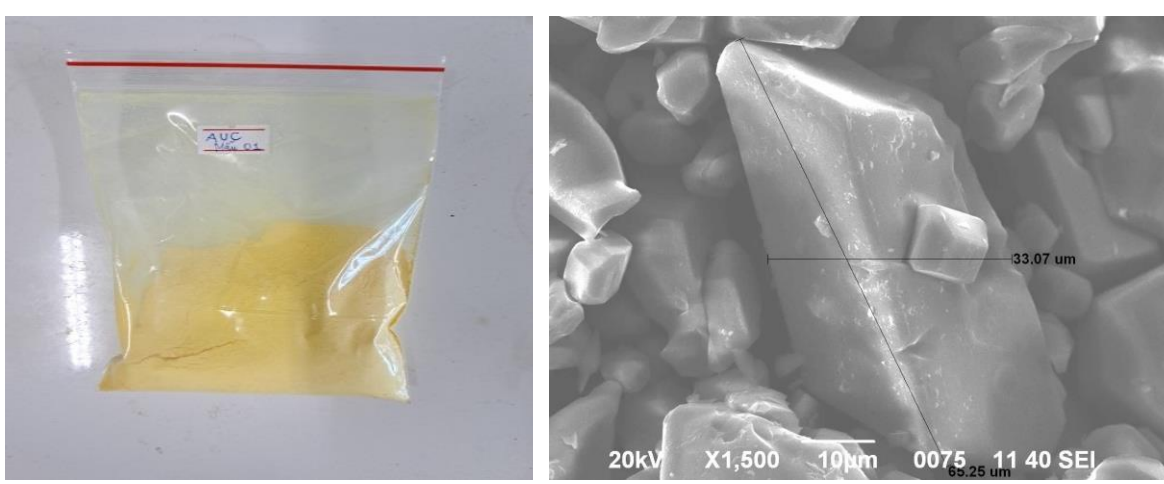


**Fig. 2.** Powder sample and SEM image of AUC

Fig. 3 shows a thermal analysis diagram TG. It is clear that the AUC crystallizes in a crystalline form, and the TG curve records a mass loss of 44.01%, consistent with the formula of AUC, $(NH_4)_4UO_2(CO_3)_3$, during thermal decomposition transforming into $UO_3$ compound according to the reaction equation:

$$(NH_4)_4UO_2(CO_3)_3 = UO_3 + 4NH_3 + 3CO_2 + 2H_2O \quad (8)$$

However, to achieve a high AUC precipitation efficiency (>96%) and large AUC particle sizes, the optimal precipitation conditions are: uranium concentration in the $UO_2F_2$ solution of 100 $gL^{-1}$, $(NH_4)_2CO_3$ precipitant concentration of 300-400 $gL^{-1}$, and a C/U molar ratio of 8. This set of conditions also represents the optimum parameters for the AUC precipitation. Our research results align entirely with the references [18-27].

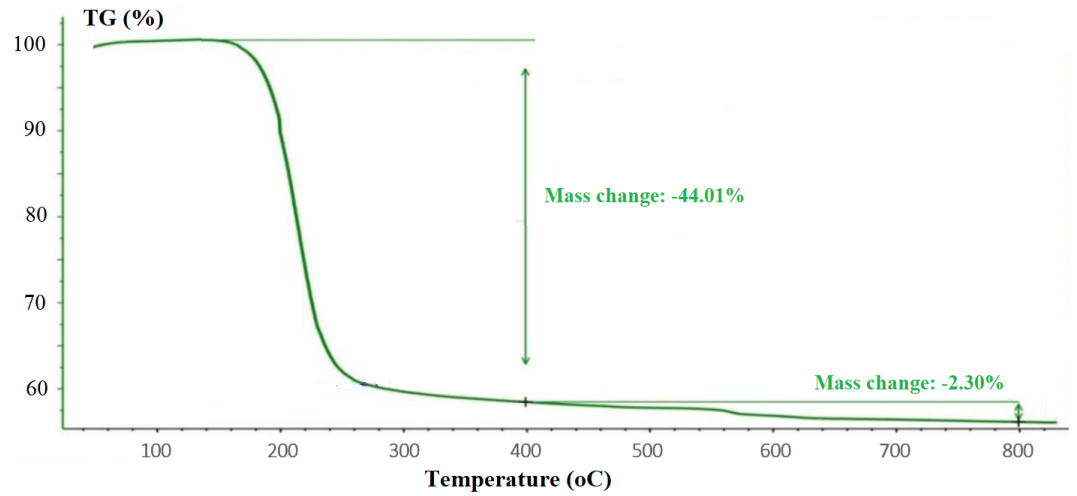


**Fig. 3.** Thermal analysis TG diagram of AUC

## B. Optimizing the ex-AUC sintering to obtain high density $U_3O_8$ powder

### *1. Determining the planning experimental region*

Based on the thermal analysis diagram in Fig. 3, it can be observed that in the temperature range of 150-400°C, the AUC transformation according to equation 8 occurs, resulting in the formation of $UO_3$ compound, corresponding to a mass loss of 44.01%. Subsequently, the transformation of $UO_3$ into $U_3O_8$ takes place according to the equation:

$$3UO_3 = 2UO_3.UO_2 + 1/2O_2 \quad (9)$$

This transformation occurs in the temperature range of 400-900°C, corresponding to a mass loss of 2.30%. According to the results of various researchers, the complete transformation of $UO_3$ into $U_3O_8$ occurs at temperatures >900°C [28-35]. Therefore, the thermal analysis results indicate that the sintering temperature for $U_3O_8$ will commence at 1000°C. According to references [28-35], the sintering for $U_3O_8$ powder is typically completed at 1400°C. In general, for a sintering, such as that for $U_3O_8$, besides temperature, factors like sintering time can also have an impact, for instance, on the density of the $U_3O_8$ powder. The sintering of uranium dioxide ceramic - $UO_2$ has been researched and reported in several papers by us [36-39]. Therefore, based on this experience, literature references, the TG curve of AUC, and experimental data, the main influencing factors have been identified as sintering temperature and sintering time, with a dependent factor being the density (in $gcm^{-3}$) of the $U_3O_8$ powder; and the planned experimental region was determined as follows: sintering temperature from 1000 to 1400°C and sintering time from 6 to 10 hours.

The Response Surface Methodology (RSM) based on the Central Composite Design (CCD) model has been employed in an empirical manner to optimize the sintering of ex-AUC $U_3O_8$ powder. Experimental setups were conducted within this experimental range. The independent variables (response) are sintering temperature (°C) and sintering time (hours), while the dependent variable is the density of the $U_3O_8$ powder ($gcm^{-3}$). The principles of the RSM-CCD method have been detailed in the referenced literature [38-39].

Table II illustrates the experimental design (planning) for the RSM-CCD model. According to this table, for the response depending on 2 variables (k=2), the number of experiments will be $2^k + 2k + n_0 = 9$ (where the number of experiments at the center $n_0$=1). The experiments on the sintering of $U_3O_8$ powder were conducted based on the designed experimental planing. The obtained results were used as input data for the MODDE 5.0 software to determine the mathematical equation

describing the density of the $U_3O_8$ powder (the density of $U_3O_8$ powder was determined according to ASTM C373-88 standards) in relation to the sintering temperature and sintering time factors (Table II).

**Table II.** Planing experimental region of RSM-CCD model

| Run | Independent variables | | | | Responses | |
|---|---|---|---|---|---|---|
| | Real values | | Coded levels | | Experimental* (Actual) ($gcm^{-3}$) | Calculated (Predicted) ($gcm^{-3}$) |
| | Sintering temperature ($X_1$) ($^oC$) | Sintering time ($X_2$) (h) | $X_1$ | $X_2$ | | |
| 1 | 1000 | 6 | -1 | -1 | 7.2 | 7.21E+00 |
| 2 | 1400 | 6 | 1 | -1 | 7.6 | 7.61E+00 |
| 3 | 1000 | 10 | -1 | 1 | 7.6 | 7.61E+00 |
| 4 | 1400 | 10 | 1 | 1 | 7.8 | 7.81E+00 |
| 5 | 1000 | 8 | -1 | 0 | 7.5 | 7.49E+00 |
| 6 | 1400 | 8 | 1 | 0 | 7.8 | 7.79E+00 |
| 7 | 1200 | 6 | 0 | -1 | 7.4 | 7.39E+00 |
| 8 | 1200 | 10 | 0 | 1 | 7.7 | 7.69E+00 |
| 9 | 1200 | 8 | 0 | 0 | 7.6 | 7.62E+00 |

### *2. Modeling the ex-AUC $U_3O_8$ sintering*

The experimental data from 9 experiments according to the experimental design are presented in Table 2. Based on these experimental results, the calculated outcomes from the MODDE 5.0 software provided the coefficients for the RSM-CCD equation:

$$Y = b_0 + \sum_{i=1}^{k} b_i X_i + \sum_{i=1}^{k} b_{ii} X_i^2 + \sum_{i,j=1(i\neq j)}^{k} b_{ij} X_i X_j \quad (10)$$

Where:

Y is the dependent response;

$b_0$ is the constant coefficient;

$b_i$, $b_{ii}$ and $b_{ij}$ are the linear, quadratic, and interaction coefficients, respectively;

$X_i$ and $X_j$ are the coded values of the independent variables;

$X_iX_j$ and $X_i^2$ represent the interaction and quadratic terms, respectively.

The values of these coefficients were listed in Table 3. The mathematical equation describing the influence of the sintering temperature ($X_1$) and sintering time ($X_2$) factors on the density of $U_3O_8$ powder (Y) is as follows:

$$Y=7.6+0.15X_1+0.15X_2 -0.08X_2^2 - 0.05X_1X_2 \quad (11)$$

**Table III.** Estimated regression coefficients for sequential model

| Source | Coefficient | Standard error | p-value | Source |
|---|---|---|---|---|
| 1 | Model ($b_0$) | 7.62222 | 0.0143444 | 1.46983e-008 |
| 2 | $X_1$ ($b_1$) | 0.15 | 0.00785674 | 0.000313798 |
| 3 | $X_2$ ($b_2$) | 0.15 | 0.00785674 | 0.000313801 |
| 4 | $X_1^2$ ($b_1^2$) | 0.016667 | 0.0136083 | 0.308059 |
| 5 | $X_2^2$ ($b_2^2$) | -0.0833338 | 0.0136083 | 0.00875428 |
| 6 | $X_{12}$ ($b_{12}$) | -0.0500001 | 0.00962251 | 0.0138468 |

The calculated data from the RSM-CCD equation is also presented in Table 2. Fig. 4 illustrates the correlation between experimental and calculated data, indicating a correlation coefficient $R^2 = 0.996$. Thus, the calculated data align well with the experimental results. The mathematical equation describing the coagulation depends on the established factors (equation 11).

The analysis of the coefficients in the RSM-CCF equation (equation 11) is detailed below:

(i) The linear coefficient contribution (impact) to the objective function (density) of the two factors, temperature and time, is equal and calculated as $b_0 + 0.15$. This means that the density of $U_3O_8$ powder will increase by 0.15 $gcm^{-3}$ when the sintering temperature rises from 1200°C to 1400°C.

(ii) The quadratic coefficient of the temperature factor is eliminated due to a large error. The quadratic coefficient of the time factor's contribution (impact) to the objective function (density) is calculated as $b_0 + 0.08$. This implies that the density of $U_3O_8$ powder will increase by 0.08 $gcm^{-3}$ when the sintering time rises from 8 hours to 10 hours.

(iii) The interaction coefficient's contribution (impact) on the objective function (density) is calculated as $b_0 + 0.05$. This means that the density of $U_3O_8$ powder will increase by 0.05 $gcm^{-3}$ when both the sintering temperature and time rise from 1200°C to 1400°C and from 8 hours to 10 hours, respectively.

From the results of the coefficient analysis, it can be observed that the influence of the sintering temperature factor is smaller than the influence of the sintering time factor. This helps quantify the impact of these factors and subsequently control the sintering.

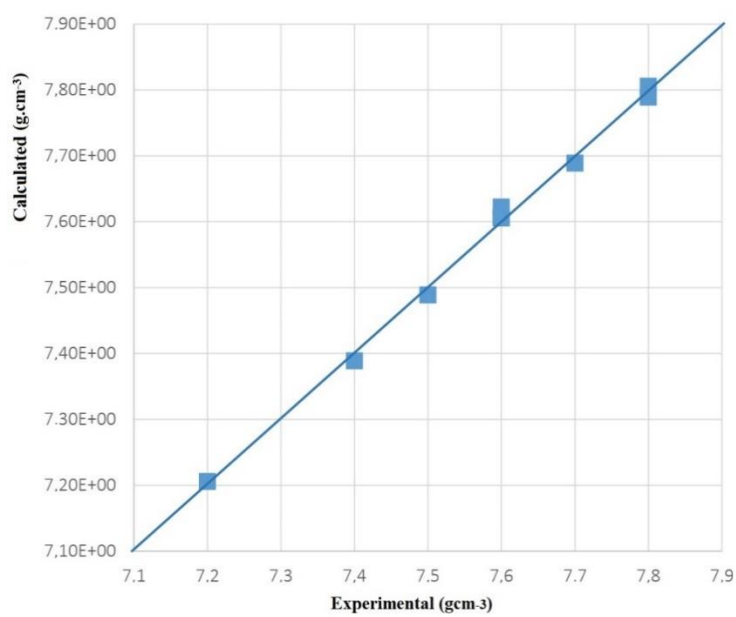


**Fig. 4.** Linear correlation between calculated and experimental values for the ex-AUC $U_3O_8$ sintering

### *3. Optimizing the ex-AUC $U_3O_8$ powder sintering*

Figure 5 provides a visual representation of the synergistic impact of temperature and sintering time on the density of $U_3O_8$ powder. The optimization results from MODDE 5.0 are presented in Table IV. Thus, through the optimization method of RSM-CCF, the sintering of $U_3O_8$ powder derived from AUC has been optimized to achieve a high-density $U_3O_8$ product. The research results have indicated that the optimal sintering temperature is 1400°C, and the optimal sintering time is 9.2 hours. Under these conditions, the density of $U_3O_8$ powder reaches the value of 7.8 $gcm^{-3}$.

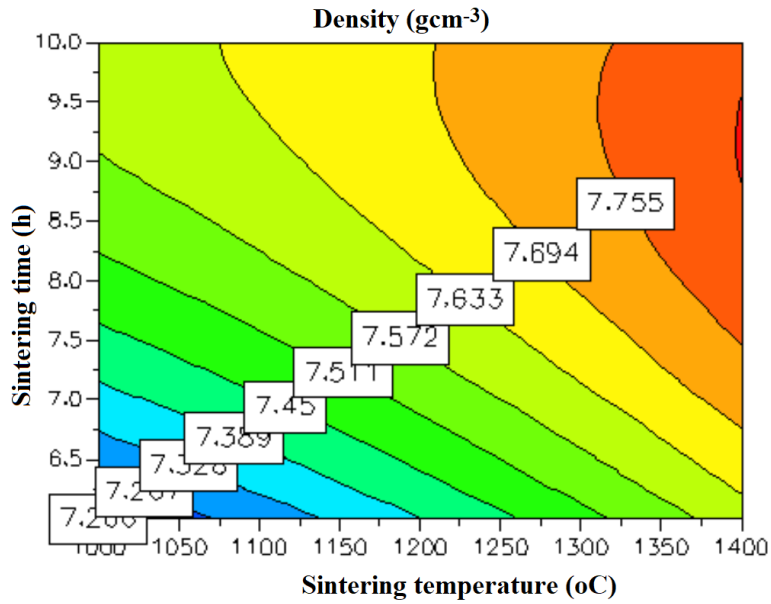


**Fig. 5.** Contours of the ex-AUC $U_3O_8$ powder density depending on sintering temperature and time

**Table IV.** Results of optimization and optimum levels of variables

| Sintering temperature (°C) | Sintering time (h) | Density ($gcm^{-3}$) |
|---|---|---|
| 1399,99 | 9.2004 | 7.8189 |
| 1399,98 | 9.1982 | 7.8189 |
| 1400 | 9.3395 | 7.8185 |
| 1400 | 9.2 | 7.8189 |
| 1400 | 9.5 | 7.817 |
| 1400 | 9.2 | 7.8189 |
| 1400 | 8.8 | 7.8156 |
| 1400 | 9.2 | 7.8189 |

### C. The flow sheet for synthesizing the high-density ex-AUC $U_3O_8$ powder

Fig. 6 showed the flow sheet for preparing the high density ex-AUC $U_3O_8$ powder product of ≥ 7.4 $gcm^{-3}$ and could be described as follows:

(i) The AUC is precipitated from a $UO_2F_2$ solution with a concentration of 100 $gL^{-1}$, using $(NH_4)_2CO_3$ precipitant agent with a concentration of 400 $gL^{-1}$ and a C/U ratio of 8; the precipitation is carried out in a stable pH environment of 8, using a 1M $NH_4OH$ buffer solution. The AUC precipitate is aged overnight, then washed with saturated $(NH_4)_2CO_3$ solution and subsequently rinsed with absolute alcohol. After the washing removes all $F^-$ ions, the AUC precipitate is dried at a temperature of 70°C for 5 hours; finally, the AUC powder product is obtained.

(ii) The AUC powder is sintered to produce a high-density $U_3O_8$ powder product. Based on mathematical equation 11, we can calculate that sintering conditions at 1200°C for more than 6 hours will result in the production of ex-AUC $U_3O_8$ powder with a density greater than 7.4 $gcm^{-3}$.

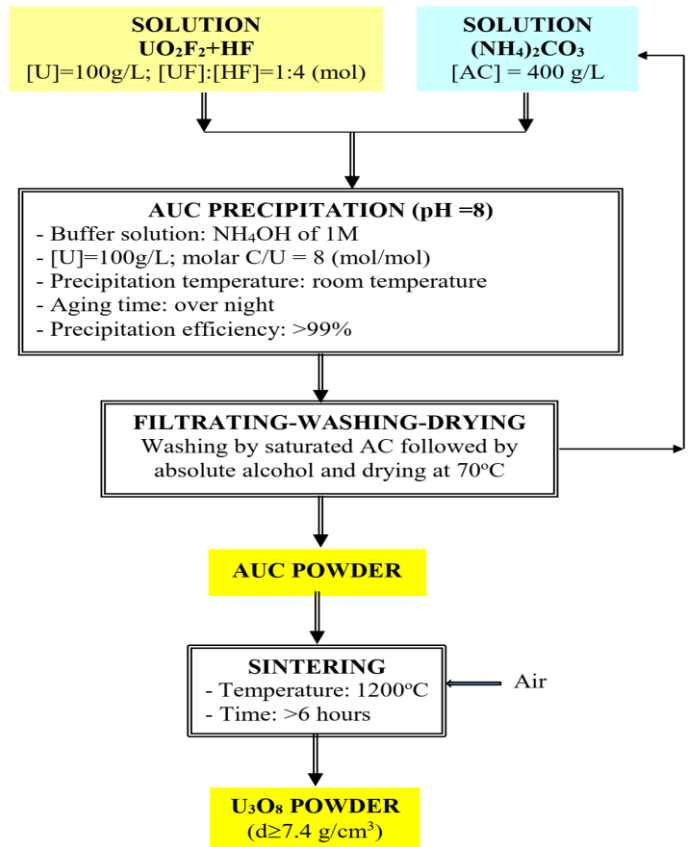


**Fig. 6.** Flow sheet for synthesizing the high density ex-AUC $U_3O_8$ powder

Table V indicates various mechanical and physical characteristics of the product. The XRD spectrum of the $U_3O_8$ sample sintered at 1200°C (Fig. 7) indicates that the structures of $U_3O_8$ samples were mostly single-phase. The XRD spectra (Fig. 7) also showed that the ex-AUC $U_3O_8$ powder is α-$U_3O_8$ with an orthorhombic structure with unit-cell parameters of a=6.682(1) Å, b=11.866(6) Å, and c=4.296(8) Å, angles of α=β=γ=90°, and a space group of *C2mm*. Previous studies have confirmed the structure of α-$U_3O_8$ [40-43]. These studies revealed that the uranium atoms in α-$U_3O_8$ are coordinated with oxygen in a 7-fold manner. Five oxygen atoms lie on the same plane, while the remaining two oxygen atoms are positioned on either side of the plane, forming a pentagon-based bipyramidal structure. The refined unit cell parameters of α-$U_3O_8$ were reported as follows: a=6.751(1) Å, b=11.978(2) Å, and c=4.1607(8) Å in the *C2mm* space group. Therefore, our studies on the structure of α-$U_3O_8$ are in good agreement with those presented in the existing literatures.

**Table V.** Characteristics of the ex-AUC $U_3O_8$ powder

| Inspection items | ex-AUC $U_3O_8$ powder | Methods |
|---|---|---|
| Density, in $10^3$kg/m$^3$ | 7.4 – 7.8 | ASTM C373-88 (Hydrostatic) |
| Ratio of O/U | 2.662 ± 0.008 | ASTM C696-99 (Gravimetry) |
| Content of F, in ppm | 8 | ASTM C696-99 (Pyrohydrolysis) |
| Content of Cl, in ppm | 23 | ASTM C696-99 (Pyrohydrolysis) |
| Content of C, in ppm | 82 | ASTM C776-06 |
| **Impurities**, in ppm | | ASTM C776-06 (ICP-MS) |
| Al | 93 | |

| | |
|---|---|
| Ca+Mg | 137 |
| Cr, Co, Th, B, Cd | below detection |
| Fe | 191 |
| Mn | 178 |
| Zn | 153 |
| Rare Earths | <1 |

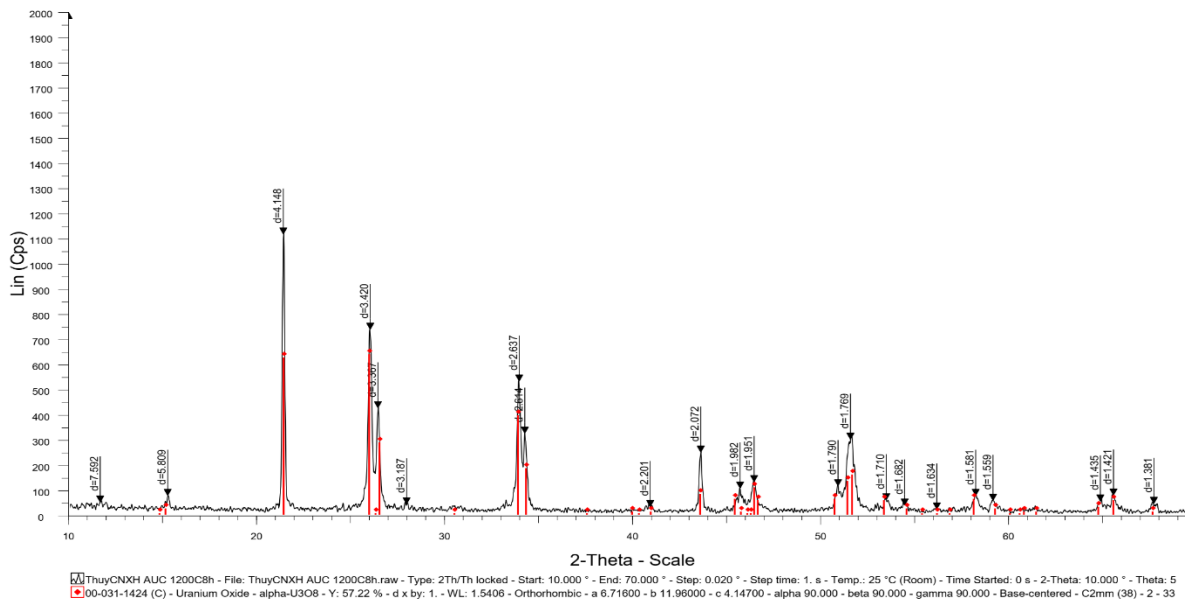


**Fig. 7.** XRD spectrum of the ex-AUC $U_3O_8$ powder

The SEM images in Fig. 8 depict the sintered ex-AUC $U_3O_8$ powder at 1200°C, showcasing spherical particles. Thus, the high-density ex-AUC $U_3O_8$ powder, which is synthesized, meets the quality requirements in terms of density and ASTM C776-06 impurity content for a nuclear material orienting to LEU nuclear fuel for research reactor.

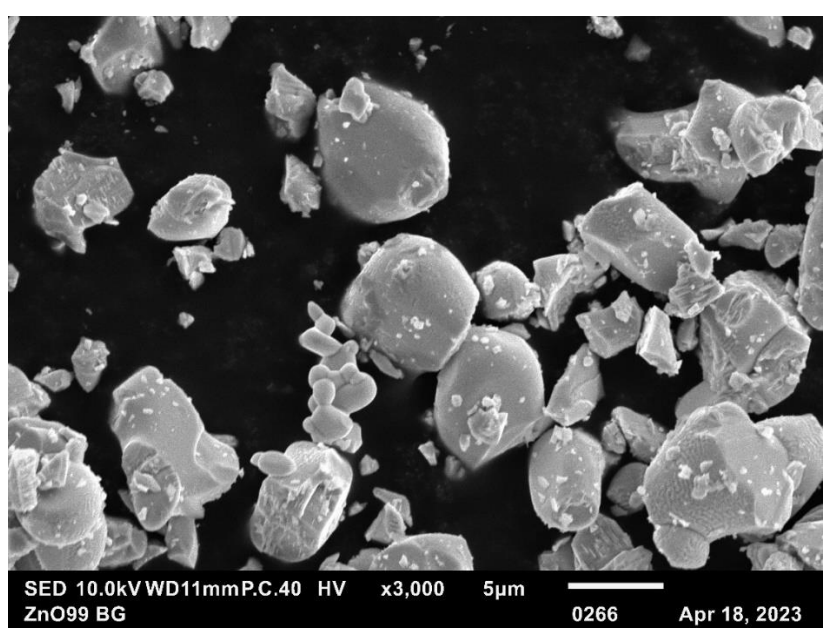


**Fig. 8.** The SEM microphotograph of the ex-AUC $U_3O_8$ powder at sintering temperature of 1200°C

## IV. CONCLUSIONS

With the aim of investigating the technical parameters for producing $U_3O_8$ powder from AUC with a density exceeding 7.4 $gcm^{-3}$, meeting the standards for oriented nuclear fuel for research reactors, the paper has identified the technical parameters of the AUC compound formation from the $UO_2F_2$+HF solution, the solution simulating the $UF_6$ hydrolysis. Subsequently, it outlines the process of transforming the AUC compound into $U_3O_8$ powder, including the technical parameters of the sintering to achieve a high-density $U_3O_8$ product.

(1) For the AUC precipitation from the $UO_2F_2$+HF solution system, the optimal technical parameters include a uranium concentration in the $UO_2F_2$ solution of 100 $gL^{-1}$, a precipitant concentration of $(NH_4)_2CO_3$ ranging from 300 to 400 $gL^{-1}$, and a C/U molar ratio of 8. Through thermal analysis (TG) and X-ray diffraction (XRD), it has been determined that the obtained AUC product is crystalline and conforms to the formula $2(NH_4)_2CO_3.UO_2CO_3$.

(2) For the sintering of $U_3O_8$ powder derived from AUC, utilizing a multi-factor optimized experimental design through the response surface methodology with central composite design (RSM-CCD). The technological parameters for the high density ex-AUC $U_3O_8$ synthesizing could be calculated from the proposed model so that the $U_3O_8$ product has the desirable density level; and the optimal technical parameters for the process have been determined as follows: a sintering temperature of 1400$^oC$ and a sintering time of 9.2 hours. The resulting $U_3O_8$ powder product achieves a density of 7.8 $gcm^{-3}$.

(3) Finally, a flow sheet for the synthesizing the high-density ex-AUC $U_3O_8$ powder has been established.

## ACKNOWLEDGEMENT

Dr. Nguyen Trong Hung expresses his sincere gratitude to the authorities of VINATOM and the MOST. This research was financially supported by the Ministry projects “Study on preparation of the high density compound $U_3O_8$ orienting to LEU nuclear fuel for research reactor” under grant No. DTCB.10/22/VCNXH.

## REFERENCES

[1]. IAEA-TECDOC 1374. Development status of metallic, dispersion and non-oxide advanced and alternative fuels for power and research reactors.

[2]. M. R. FINLAY and M. I. RIPLEY. A New Fuel for Research Reactors. https://inis.iaea.org/collection/NCLCollectionStore/_Public/33/034/33034319.pdf.

[3]. R.G. Muranaka. Conversion of research reactors to low-enrichment uranium fuels. IAEA BULLETIN, VOL.25, No.1. https://www.iaea.org/sites/default/files/25105381821.pdf.

[4]. Copeland, G. And Martin, M. Development of High - Uranium Loaded $U_3O_8$ - Al Fuel Plates. Nuclear Technology. 1982, Vol. 56.

[5]. Nazaré, S. New Low Enrichment Dispersion Fuels for Research Reactors Prepared by PM-Techniques. J. Nucl. Mat. 1984 (124) p. 14.

[6]. R. W. Knight et al (1968). Fabrication procedures for manufacturing high flux isotope reactor fuel elements. U.S. ATOMIC ENERGY COMMISSION

[7]. G. M. Adamson (1969). Fabrication procedures for the initial high flux isotope reactor fuel elements. U.S. ATOMIC ENERGY COMMISSION

[8]. A. M. Saliba-Silva et al. Research Reactor Fuel Fabrication to Produce Radioisotopes. Chapter, October 2011.

[9]. W. J. Werner and J. E. Barkman (1967). Characterization and production of $U_3O_8$ for the high flux isotope reactor. U.S. ATOMIC ENERGY COMLCSSION.

[10]. G. L. Copeland and M. M. Martin (1960). Fabrication of high-uranium-loaded $U_3O_8$ developmental fuel plates. Oak Ridge National Laboratory.

[11]. R. W. Knight, J. Binns, and G. M. Adamson, Jr. (1968). fabrication procedures for manufacturing high flux isotope reactor fuel elements. U.S. ATOMIC ENERGY COMLCSSION.

[12]. Nguyen Trong Hung (2007). Vietnam's yellow cake refining achieving nuclear purity through the TBP solvent extraction. Doctoral thesis, VINATOM.

[13]. Le Ba Thuan, Nguyen Trong Hung, et al. (2000). Research on Vietnam's yellow cake refining achieving certain nuclear purity criteria, using the TBP solvent extraction. Final report on Ministry project (code CB-98/05), VINATOM.

[14]. Eung Ho Kim, Cheong Song Choi, Jin Ho Park, Seon Gil Kwon, In Soon Chang (1994). A study on morphology and chemical composition of precipitates produced from $UO_2(NO_3)_2$-$(NH_4)_2CO_3$ solution, Journal of Nuclear Materials, 209(3), 301-305.

[15]. A Boualia, A Mellah (1989). Précipitation de l'AUC par $NH_3$ et $CO_2$ à partir des solutions de nitrate d'uranyle. Precipitation of AUC by $NH_3$ and $CO_2$ from an uranyl nitrate solution. Hydrometallurgy 21(3), 331-344.

[16]. Rofail N.H. (1994). Infrared and X-ray diffraction spectra of ammonium uranyl Carbonate. Materials Chemistry and Physics, 36, 241-245.

[17]. Graziani R., Bombieri G. and Forsellini E. (1972). Crystal Structure of Tetra-mmonium Uranyl Tricarbonate. Journal of the Chemical Society, Dalton Transactions 19, 2059-2061.

[18]. Tae-Joon Kim, Kyung-Chai Jeong, Jin-Ho Park, In-Soon Chang, Cheong-Song Choi (1994). Crystallization characteristics of ammonium uranyl carbonate (AUC) in ammonium carbonate solutions. Journal of Nuclear Materials, 209, 306-314.

[19]. H. Tel, M. Eral (1996). Investigation of production conditions and powder properties of AUC. Journal of Nuclear Materials, 231, 165.

[20]. A. Marajofsky, L. Perez, J. Celora (1991). On the dependence of characteristics of powders on the AUC process parameters. Journal of Nuclear Materials, 178, 143-151.

[21]. C. S. Choi, J. H. Park, E. H. Kim, H. S. Shin, I. S. Chang (1988). The influence of AUC powder characteristics on $UO_2$ pellets. Journal of Nuclear Materials, 153, 148.

[22]. S. Chegrouche, A. Kebir (1992). Study of ammonium uranyl carbonate re-extraction-crystallization process by ammonium carbonate. Hydrometallurgy, 28(2), 135-147.

[23]. Maw-Chwain Lee, Chung-Jyi Wu (1991). Conversion of $UF_6$ to $UO_2$: A quasi-optimization of the ammonium uranyl carbonate process. Journal of Nuclear Materials, 185(2), 190-201.

[24]. Yi-Ming Pan, Che-Bao Ma, Nien-Nan Hsu (1981). The conversion of $UO_2$ via ammonium uranyl carbonate: Study of precipitation, chemical variation and powder properties. Journal of Nuclear Materials, 99(2-3), 135-147.

[25]. Kan-Sen Chou, Ding-Yi Lin, Mu-Chang Shieh (1989). Precipitation studies of ammonium uranyl carbonate from $UO_2F_2$ solutions. Journal of Nuclear Materials, 165(2), 171-178.

[26]. M.H. Sadeghi, M. Outokesh, M. Habibi Zare (2020). Production of high quality ammonium uranyl carbonate from "uranyl nitrate + carbonate" precursor solution. Progress in Nuclear Energy, 122, 103270.

[27]. P. Govindan, A. Palamalai, T. Vasudevan, K. S. Vijayan, R.V. Subba Rao, M. Venkataraman, R. Natarajan (2012). Ammonium uranyl carbonate (AUC) based process of simultaneous partitioning and reconversion for uranium and plutonium in fast breeder reactors (FBRs) fuel reprocessing, Journal of Radioanalytical and Nuclear Chemistry, 295(1).

[28]. V. Baran, F. Skvor, V. Vosecek (1984). Formation of the Ammonium-Uranyl-Carbonate Complexes of the Type ($NH_4[UO_2(CO_3)_3]$

Prepared by Precipitative Reextraction. Inorganica Chimica Acta, 81, 83-89.

[29]. L. Hälldahl, M. Nygren (1986). Thermal analysis studies of the reactions occurring during the decomposition of ammonium uranyl carbonate in different atmospheres. Journal of nuclear materials, 138, 99-106.

[30]. L. Hälldahl, M. Nygren (1984). TG, DSC, X-ray and electron diffraction studies of intermediate phases in the reduction of ammonium uranyl carbonate to $UO_2$. Thermochimica Acta, 72(1-2), 213-218.

[31]. B.S. Girgis, N.H. Rofail (1992). Decomposition-reduction stages of ammonium uranyl carbonates under different atmospheres. Thermochimica Acta, 196 (1-3), 105-115.

[32]. S. Korichi, F. Mernache, F. Benaouicha, N. Aoudia, A. Amrane, S. Hadji (2017). Thermal behavior and kinetic modeling of $(NH_4)_4UO_2(CO_3)_3$ decomposition under non-isothermal conditions. J. Radioanal. Nucl. Chem., 314, 923–934.

[33]. Korichi Smain , Aoudia Nacera, Benelmaddjat Hanane, Kaci Smina and Ousmaal Nafissa (2019). Kinetic studies of isothermal decomposition of $(NH_4)_4UO_2(CO_3)_3$ to uranium oxide. Progress in Reaction Kinetics and Mechanism, 45, 1-12.

[34]. E.H. Kim, J.J. Park, J.H. Park, I.S. Chang, C.S. Choi, S.D. Kim (1994). Thermal decomposition kinetics of ammonium uranyl carbonate. Journal of Nuclear Materials, 209(3), 294-300.

[35]. A. Mellah, S. Chegrouche, M. Barkat (2007). The precipitation of ammonium uranyl carbonate (AUC): Thermodynamic and kinetic investigations. Hydrometallurgy, 85, 163–171.

Flynn, J.H. (1983). The isoconversional method for determination of energy of activation at constant heating rates. Journal of Thermal Analysis, 27, 95-102.

[37]. Nguyen Trong Hung, Thuan L.B., Thanh T.C., Nhuan H., Khoai D.V., Tung N.V., Lee J.Y., Jyothi R.K., 2018. Modeling the $UO_2$ ex-AUC pellet process and predicting the fuel rod temperature distribution under steady-state operating condition. Journal of Nuclear Materials 504, 191–197.

[38]. Nguyen Trong Hung, Thuan L.B., Tung N.V, Thuy N.T., Lee J.Y., Jyothi R.K., 2017. The $UO_2$ ex-ADU powder preparation and pellet sintering for optimum efficiency: experimental and modeling studies. Journal of Nuclear Materials 496, 177–181.

[39]. Nguyen Trong Hung, Thuan L.B., Khoai D.V., Lee J.Y., Kumar J.R., 2016. Modeling conversion of ammonium diuranate (ADU) into uranium dioxide ($UO_2$) powder. Journal of Nuclear Materials 479, 483-488.

[40]. Nguyen Trong Hung, Thuan L.B., Khoai D.V., Lee J.Y., Kumar J.R., 2016. Brandon mathematical model describing the effect of calcination and reduction parameters on specific surface area of $UO_2$ powders. Journal of Nuclear Materials 474, 150-154.

[41]. R.E. Rundle, N.C. Baenziger, A.S. Wilson, R.A. McDonald (1948). The Structures of the Carbides, Nitrides and Oxides of Uranium. J. Am. Chem. Soc., 70, 99-105.

[42]. R. Herak, B. Jovanovic (1969). On the existence of $\delta$-$U_3O_8$. Inorg. Nucl. Chem. Lett., 5, 693-697.

[43]. B.O. loopstra (1964). Neutron Diffraction Investigation of $U_3O_8$. Acta Cryst., 17, 651-654.

[44]. Zhang F.X., Lang M., Wang J.W., Li W.X., Sun K., Prakapenka V., Ewing R.C., 2014. High-pressure $U_3O_8$ with the fluorite-type structure. Journal of Solid State Chemistry 213, 110-115.